A Novel Type of Equipment for Reactive Distillation: Model Development, Simulation, Sensitivity and Error Analysis

Erik von Harbou
Dept. of Mechanical and Process Engineering, Laboratory of Engineering Thermodynamics, University of Kaiserslautern, Kaiserslautern, Germany

Markus Schmitt and Christoph Großmann
Global Process Technology, BASF SE, Ludwigshafen, Germany

Hans Hasse
Dept. of Mechanical and Process Engineering, Laboratory of Engineering Thermodynamics, University of Kaiserslautern, Kaiserslautern, Germany

DOI 10.1002/aic.13947
Published online November 15, 2012 in Wiley Online Library (wileyonlinelibrary.com).

A simulation study of heterogeneously catalyzed reactive distillation experiments carried out with the D + R tray, a novel type of laboratory equipment, is presented. One advantage of the D + R tray is that reaction and distillation are alternating stage-wise, in a well-defined way that can be modeled straightforwardly. An equilibrium stage model is used to describe the distillation and a plug flow reactor model to describe the catalyst bed reactors. The model parameters are derived from a systematic experimental characterization of the D + R tray both as a reactor and as a distillation unit. A validated physicochemical fluid property model is used. The primary experimental data are reconciled. Results from the predictive simulations are in good agreement with the experimental results. The influence of errors in the input parameters on the simulation results is investigated by means of a sensitivity and error analysis. © 2012 American Institute of Chemical Engineers *AIChE J,* 59: 1533–1543, 2013
Keywords: reactive distillation, tray, modeling and simulation, data reconciliation, sensitivity analysis

Introduction

Reactive distillation (RD) has received much attention in the last years, as it has various potential advantages compared with conventional processes comprising a reactor followed by distillation. Especially, for reaction systems in which the maximum conversion is limited by chemical equilibrium, the application of RD can be beneficial. The *in situ* separation of the products can enhance the conversion and selectivity compared with conventional reactors by forcing the reaction into the direction of the products. On the other hand, an undesired increase of side product formation may occur. A detailed discussion of the benefits and constraints of RD is given, for example, by Taylor and Krishna.[1] The reaction can be catalyzed either heterogeneously or homogeneously. Heterogeneously catalyzed RD (HCRD), however, has some important advantages. The position and size of the reactive zone in the column can be chosen freely. Furthermore, the separation and recycling of the catalyst can be avoided. The long list of industrially relevant RD processes given by Hiwale et al.[2] shows that RD is a well-established technique today. For that reason, RD is often considered as an option in industrial process development.[3] In that development, laboratory tests of RD are necessary, as they provide essential information for the modeling and scale-up of the process.[4] Basically, there are two different types of internals for HCRD experiments: packings and trays. Reviews on hardware selection for RD are given, for example, by Krishna[5] and Dörhöfer.[6] Packed columns with catalyst in gauze pockets are not only often favored in industrial applications[5] but also widely used for laboratory tests (e.g., Buchaly et al.,[7,8] Hanika et al.,[9] Pöpken et al.,[10] Steinigeweg and Gmehling,[11] Schmitt et al.,[12] and Parada[13]). These structured packings, however, have the disadvantage that any change of the catalyst is not only costly but also time-consuming, as it requires the dismantling of the column and often even the purchase of a new set of packings. For that reason, typically neither the type of catalyst nor its amount is varied in HCRD experiments using structured packings. Especially, in laboratory scale, a more flexible handling of the catalyst is desirable, as it facilitates swift investigations of several process options and types of catalysts. Furthermore, it is well known that undesired flow characteristics, such as stagnant zones and bypassing, can occur in HCRD packings.[14]

To overcome these disadvantages, new equipment for laboratory studies of HCRD based on trays was developed by Adrian et al.[15] It is called D + R tray, as it consists of a distillation tray (D), which is a conventional bubble cap tray, and a reactive section (R), which is filled with the catalyst. The novel equipment is designed, so that the catalyst can be easily changed and its amount can be flexibly chosen. Details on the design of the D + R tray were first presented

Correspondence concerning this article should be addressed to E. von Harbou at erik.vonharbou@mv.uni-kl.de.

by Schmitt et al.[16] In following work, a thorough characterization of the D + R tray both as a distillation unit and as a reactor was carried out by Schmitt et al.[16] and von Harbou et al.[17] including measurements of the separation capacity and the residence time distribution. Following, the D + R tray was used in extensive experimental HCRD studies both for the production of *n*-butyl acetate and for the production of *n*-hexyl acetate as reported by von Harbou et al.[17]

This article completes the investigations of the D + R tray by a simulation study. First, the development of a simple and physically reasonable model for the description of HCRD with the D + R tray is presented that is based on the careful characterization of the D + R tray as a distillation unit and as reactor. Second, the process model together with a thoroughly validated model of the physicochemical fluid properties of the studied systems is implemented in the process simulator Chemasim, which is an in-house tool of BASF SE (Ludwigshafen, Germany). The HCRD model is validated by comparison of the predictive simulation results to the results of the HCRD experiments both for the production of *n*-butyl acetate and for the production of *n*-hexyl acetate.

Prior to the simulations, the primary experimental data are subjected to a data reconciliation procedure. As the experimental data are inevitably corrupted by measurement errors, which may occur during the experiments or during the analysis of the samples, typically neither the total mass balance nor the component mass balances or the stoichiometry are satisfied if redundancy exists in the measurements. To get a consistent data set and to enable a meaningful comparison of the experimental data and the simulation result, a data reconciliation procedure is carried out. The benefit of data reconciliation and its implementation for real processes has been repeatedly demonstrated, for example, by Schladt and Hu[18] for an industrial distillation process or by Buchaly et al.[8] and Keller et al.[19] for pilot-plant scale RD processes.

The model validation is complemented by a sensitivity and error analysis that investigates the influence of errors in the input parameters on the simulation results. This sensitivity and error analysis is important for a meaningful validation of the model, as it enables to assess the unavoidable differences between the simulation and experimental results.

Chemical Systems

n-*Butyl acetate system*

n-Butyl acetate (ButAc) is produced by the reversible, acid-catalyzed liquid-phase esterification of 1-butanol (ButOH) and acetic acid (HAc) with water (H_2O) as an additional product (see Reaction I). In the experiments carried out by von Harbou et al.,[17] the strongly acidic surface-sulfonated ion-exchange resin Amberlyst 46 (Rohm and Haas) was used as solid catalyst.

$$\underset{\text{1-butanol}}{C_4H_9{-}OH} + \underset{\text{acetic acid}}{CH_3{-}COOH} \overset{H^+}{\rightleftharpoons} \underset{\textit{n}\text{-butyl acetate}}{CH_3{-}COO{-}C_4H_9} + \underset{\text{water}}{H_2O} \quad \text{(I)}$$

Under the conditions present during the HCRD experiments of *n*-butyl acetate, mainly the formation of two side products, dibutyl ether (DBE) and 2-butanol (2-ButOH), was observed. According to Blagov et al.,[20] who carried out a comprehensive investigation of the reaction network, 2-butanol is formed by the isomerization of 1-butanol (cf. Reaction II).

$$\underset{\text{1-butanol}}{C_4H_9{-}OH} \overset{H^+}{\rightleftharpoons} \underset{\text{2-butanol}}{C_2H_5{-}CHOH{-}CH_3} \quad \text{(II)}$$

Furthermore, 1-butanol can react by condensation to dibutyl ether and water (cf. Reaction III).

$$\underset{\text{1-butanol}}{2C_4H_9{-}OH} \overset{H^+}{\rightleftharpoons} \underset{\text{dibutyl ether}}{C_4H_9{-}O{-}C_4H_9} + \underset{\text{water}}{H_2O} \quad \text{(III)}$$

The formation rate of additional side products is by orders of magnitude lower than the formation rate of the main products (butyl acetate and water), and hence these side products are neglected in this work. Furthermore, Parada[13] showed that the autocatalytic reaction of butanol with acetic acid is negligible compared with the heterogeneously catalyzed reaction.

The butyl acetate system shows strong liquid- and also vapor-phase nonidealities. A large miscibility gap and several homogeneous and heterogeneous azeotropes are present. Furthermore, acetic acid dimerization takes place in the vapor phase.[13,21]

n-*Hexyl acetate system*

n-Hexyl acetate (HexAc) is formed by the acid-catalyzed esterification of 1-hexanol (HexOH) with acetic acid (HAc) and water as an additional product (see Reaction IV). The conversion of this reaction is limited by chemical equilibrium. In the experiments carried out by von Harbou et al.,[17] the strongly acidic and fully sulfonated ion-exchange resin Amberlyst CSP2 (Rohm and Haas) was used as solid catalyst.

$$\underset{\text{1-hexanol}}{C_6H_{13}{-}OH} + \underset{\text{acetic acid}}{CH_3{-}COOH} \overset{H^+}{\rightleftharpoons} \underset{\textit{n}\text{-hexyl acetate}}{CH_3{-}COO{-}C_6H_{13}} + \underset{\text{water}}{H_2O} \quad \text{(IV)}$$

Under the conditions present in the HCRD experiments of *n*-hexyl acetate, mainly two side products, dihexyl ether (DHE) and 1-hexene (HEN), were detected. According to Schmitt and Hasse,[22] these side products are formed via the Reactions V–VII.

$$\underset{\text{1-hexanol}}{2C_6H_{13}{-}OH} \overset{H^+}{\rightleftharpoons} \underset{\text{dihexyl ether}}{C_6H_{13}{-}O{-}C_6H_{13}} + \underset{\text{water}}{H_2O} \quad \text{(V)}$$

$$\underset{\text{1-hexanol}}{C_6H_{13}{-}OH} \overset{H^+}{\rightarrow} \underset{\text{1-hexene}}{C_6H_{12}} + \underset{\text{water}}{H_2O} \quad \text{(VI)}$$

$$\underset{\textit{n}\text{-hexyl acetate}}{CH_3{-}COO{-}C_6H_{13}} \overset{H^+}{\rightleftharpoons} \underset{\text{1-hexene}}{C_6H_{12}} + \underset{\text{acetic acid}}{CH_3{-}COOH} \quad \text{(VII)}$$

The formation rate of additional side products is by orders of magnitude lower than the formation rate of the main products (hexyl acetate and water), and hence these side products are neglected in this work. Furthermore, Schmitt and Hasse[22] showed that the autocatalytic reaction of hexanol with acetic acid is negligible compared with the heterogeneously catalyzed reaction.

Similar to the butyl acetate system, the hexyl acetate system shows strong liquid- and vapor-phase nonidealities with several homogeneous and heterogeneous azeotropes and a large miscibility gap. Furthermore, acetic acid dimerization takes place in the vapor phase.[23]

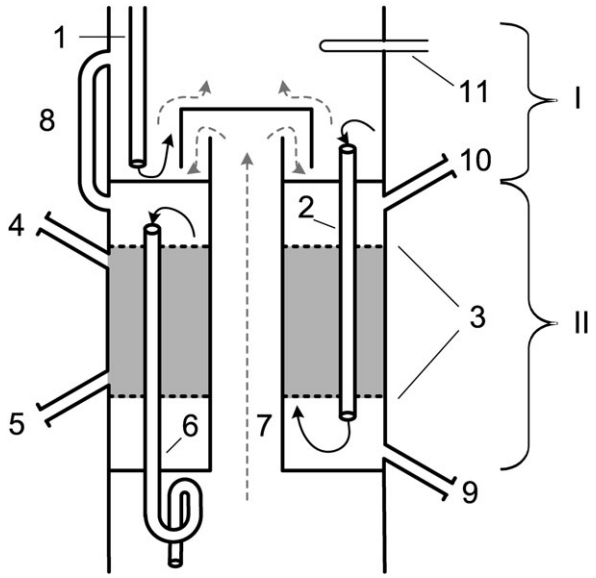

Figure 1. Schematic drawing of a D + R tray.

(I) Distillation section (D), (II) reactive section (R), (1), (2) downcomers, (3) sieves, (4) upper catalyst port, (5) lower catalyst port, (6) downcomer, (7) gas chimney, (8) venting pipe, (9) sampling port before the catalyst bed, (10) sampling port after the catalyst bed, and (11) temperature measurement. The gray area indicates the catalyst bed.

Experiments

The D + R tray

A detailed description of the D + R tray is given by Schmitt et al.[16] The D + R tray for laboratory scale HCRD studies is depicted schematically in Figure 1. It consists of two parts, namely, a standard bubble cap distillation tray (I) and a catalyst bed reactor (reactive section) mounted below (II). In the column, the liquid coming from above flows through the downcomer (1) onto the distillation tray (I) (see solid arrows in Figure 1). The downcomer (2) connects the distillation tray (I) with the inlet zone of the catalyst bed. From there, the liquid flows upward through the catalyst bed (gray area). Two sieves (3) immobilize the catalyst in the reactive section. The liquid leaves the reactive section in the upper part through the downcomer (6) to the next column section. The vapor bypasses the reactive section and flows directly upward through the gas chimney (7) from distillation tray to distillation tray (see dashed arrows in Figure 1). Thus, the vapor is never in contact with the catalyst bed.

Reactive distillation experiments

A detailed description of the experimental set-ups and procedures is given by von Harbou et al.[17] The experimental set-ups used for the two test systems are depicted in Figure 2. Both set-ups are quite similar. The reactive zone consists of eight D + R trays as described in the previous section. Below the reactive zone, a stripping zone is mounted containing 1.0 m of the noncatalytic structured packing Sulzer CY. In the HCRD experiments of butyl acetate, the column is additionally equipped with a rectifying zone containing 0.5 m of the noncatalytic structured packing Sulzer CY. Because of the heteroazeotropic behavior of the two test systems, phase separation occurs upon condensation. Thus, a decanter is installed after the condenser to split the distillate in an organic and an aqueous phase. The aqueous phase is withdrawn (S7), whereas the organic phase is fed back into the column (S8). To prevent the accumulation of low-boiling by-products such as 1-hexene during the synthesis of hexyl acetate, a small fraction of the organic phase is purged (S10). The acetate is enriched in the stripping zone and is withdrawn at the bottom (S3). For the HCRD experiments of butyl acetate, a one-feed-design is used with the upmost D + R tray as feed stage. For the HCRD experiments of hexyl acetate, however, a two-feed-design is used. In this case, 1-hexanol (S1) and acetic acid (S2) are fed at the upper and the lower end of the reactive zone, respectively, resulting in a counter-current flow of the reactants in the column.

Data reconciliation

The aim of data reconciliation is to make minor adjustments to the measured values, so that obvious physical constraints are satisfied. Mathematically, data reconciliation is a constrained optimization problem. In this work, all measured mass flows (input, output, and reflux) and the measured mass fractions are reconciled. Additionally, the data reconciliation procedure determines the unmeasured mass flows of the vapor stream (S4), the condensate stream (S5), and the organic phase (S9). Furthermore, the unknown extents of the Reactions I–III (butyl acetate system) and of the Reactions IV–VII (hexyl acetate system) are determined by the data reconciliation procedure, so that the stoichiometry of the given reaction system is satisfied. The differences between the measured mass flows and the reconciled mass flows are typically below 5 g/h, which is less than 0.5%. The differences between the measured and the reconciled mass flow of the bottom product stream (S3), however, is higher. For the hexyl acetate system, it is maximal 24 g/h but still less than 1%. For the butyl acetate system, it is maximal 40 g/h but still less than 2%. Furthermore, the data of each experiment were tested for gross errors by the data reconciliation procedure. For none of the HCRD experiments carried out by von Harbou et al.[17] a gross error was detected. As an example, Table 1 shows a comparison between the measured and reconciled main component mass flows for the HCRD experiment Hex03.[17] The adjustments of the main components streams, which are necessary to fulfil the physical constraints, are generally small, which illustrates the quality of

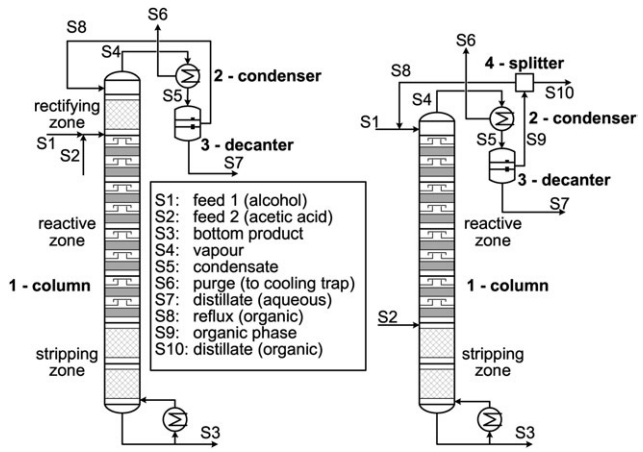

Figure 2. Flow diagram of the reactive distillation experiments.

Left side: synthesis of *n*-butyl acetate. Right side: synthesis of *n*-hexyl acetate.

Table 1. Comparison of the Measured and Reconciled Main Component Mass Flows of All Input and Output Streams from the HCRD Experiment Hex03

	Component Mass Flow (g/h)			
	HexOH	HAc	HexAc	H_2O
Feed 1 (S1)				
Meas.	1851.57	1.70	0.00	0.83
Recon.	1856.84	2.15	0.19	1.09
Feed 2 (S2)				
Meas.	0.00	1109.15	0.00	0.91
Recon.	0.02	1099.53	0.00	0.91
Product (S3)				
Meas.	144.05	0.66	2354.45	0.36
Recon.	143.03	0.50	2355.11	0.06
Purge (S6)				
Meas.	0.00	0.20	0.00	1.21
Recon.	0.00	0.21	0.00	1.21
Distillate (aq.) (S7)				
Meas.	3.65	103.30	0.37	292.45
Recon.	3.60	103.21	0.34	292.24
Distillate (org.) (S10)				
Meas.	25.59	10.93	14.58	5.34
Recon.	25.58	10.93	14.58	5.34

the primary experimental data. The complete data (measured and reconciled) of all streams and all components are given by von Harbou.[24] In the following, only the reconciled values of the total mass flows, the component mass flows, and the concentrations of all components in all streams S1–S10 (cf. Figure 2) are used and not the primary experimental data. The data reconciliation procedure is described in detail in the Appendix.

Development of the Model

Model of the D + R tray

Due to the special design of the D + R tray, reaction and distillation are alternating stage-wise, in a well-defined way. This strict separation of distillation and reaction enables the precise characterization of the D + R tray both as a reactor and as a distillation unit. For this reason, the D + R tray can be modeled straightforwardly. As described in "The D + R tray" section, the D + R tray consists of a standard bubble cap distillation tray and a catalyst bed reactor. The distillation tray is modeled with the well-known stage concept that assumes vapor–liquid equilibrium on each stage (VLE stage). The separation capacity of the distillation tray is accounted for by the Murphree stage efficiency. Details about the VLE stage concept including the stage efficiency are given, for example, by King.[25] The catalyst bed reactor is incorporated as a side reactor through which the liquid flows when it passes from one distillation tray down to the next. Schmitt et al.[16] proved that the catalyst bed reactor shows basically plug flow characteristics. The plug flow reactor (PFR) is modeled as a series of continuous stirred tank reactors (CSTRs). The number of CSTRs, N_{CSTR}, is estimated from the experimentally determined Bodenstein number Bo[16] using Eq. 1 given by Levenspiel.[26]

$$N_{CSTR} \approx \frac{Bo}{2} \tag{1}$$

Thus, based on the data of Schmitt et al.,[16] in this work, the number of CSTRs is set to 30. As the liquid, which enters the reactors, is in boiling condition and its boiling point is reduced with proceeding reaction in both test systems (under isobaric conditions), vaporization may occur in the series of CSTRs. As a consequence, the final model of the catalyst bed is a cocurrent adiabatic series of VLE-CSTRs. A schematic drawing of the D + R tray model is depicted in Figure 3. As the model of the D + R tray consists only of standard models, which are widely used for process simulations, the D + R tray model can be easily implemented in commercial process simulators.

Model of the HCRD set-up

The HCRD column is modeled as a single distillation column divided into the stripping, the rectifying, and the reactive zone (cf. Figure 2). The noncatalytic packings installed in the stripping and in the rectifying zone of the column are described by the equilibrium stage model. The number of equilibrium stages is chosen according to the number of theoretical stages per meter (NTSM) determined independently and the height of the packings as specified by von Harbou et al.[17] The reactive zone contains eight D + R trays. Each D + R tray is modeled as described in "Model of the D + R tray" section. Both the condenser and the reboiler are represented by an equilibrium stage. The decanter is described by a liquid–liquid equilibrium (LLE) stage model. Schmitt[27] showed that this model is able to predict the concentrations of the aqueous and the organic phase as well as the phase split with sufficient accuracy for the hexyl acetate system. Because adiabatic conditions were established during the experiments by means of heating jackets, no heat losses are considered in the model.

Model of the physicochemical properties

The model of the HCRD set-up described earlier requires a physicochemical property model. That model is described in detail by Parada[13] for the butyl acetate system and by Schmitt[27] for the hexyl acetate system. An overview of the used property submodels and the corresponding references is given in Table 2. The thermophysical data of the pure components comprises the vapor pressure, the heat capacity of the liquid, the enthalpy of vaporization, and the dimerization equilibrium constant of acetic acid. The liquid-phase nonidealities of the mixtures are described using G^E-models (the UNIQUAC model for the butyl acetate system and the NRTL model for the hexyl acetate system). The pressure dependence of the chemical potential is negligible. In both test systems, different parameter sets are used to describe the vapor–liquid equilibria and the liquid–liquid equilibria. The gas phase is assumed to be ideal, except for the dimerization of acetic acid, which is modeled by the chemical theory. The rate of the butyl acetate main reaction (cf. Reaction I) was measured by Parada[13] using a laboratory plug flow reactor. The rate of the hexyl acetate main reaction (cf. Reaction

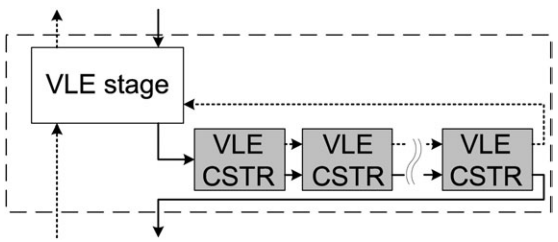

Figure 3. D + R tray model including the flow path of the liquid (solid arrows) and of the vapor (dashed arrows) and the catalyst bed (gray area).

Table 2. Overview of the Used Submodels of the Physicochemical Properties and the Corresponding References

Test System	Butyl Acetate	Hexyl Acetate
Vapor pressure	Extended Antoine Grob and Hasse[21]	Antoine Schmitt and Hasse[23]
Dimerization (HAc)	Temperature correlation equilibrium constant Gmehling and Kolbe[28]	
Enthalpy of vaporization	DIPPR equation 106 BASF*	
Heat capacity (liquid)	Polynomial BASF*	
G^E-models		
VLE	UNIQUAC Parada[13]	NRTL Schmitt and Hasse[23]
LLE	UNIQUAC Grob and Hasse[21]	NRTL Schmitt and Hasse[23]
Chemical equilibrium	Temperature correlation Parada[13]	Schmitt and Hasse[22]
Rate of reaction	Pseudohomogeneous, activity based Parada[13]	von Harbou[24]
Enthalpy of reaction	Parada[13]	Schmitt and Hasse[22]

*Taken from BASF data banks.

IV) was measured by Schmitt and Hasse[22] using a laboratory plug flow reactor and by von Harbou[24] using a laboratory CSTR. The reaction kinetics are modeled in both systems using a pseudohomogeneous approach.[13,22,24] In order to be thermodynamically consistent, the models are activity based, and the independently determined chemical reaction equilibria are taken into account. The enthalpy of the liquid phase of the pure component at 0°C is normalized to zero. The standard enthalpy of reaction is set according to Parada[13] for the butyl acetate system and Schmitt and Hasse[22] for the hexyl acetate system. Note, that despite the quite small values for the enthalpies of reaction, it is important to model them accurately as otherwise an unrealistically large temperature change in the adiabatic reactor may result.

Simulations

Input parameters

For the simulations, temperature (and pressure), and the component mass flows of all feed streams (S1 and S2 in Figure 2) as well as the pressure at the top of the column and the pressure loss along the column are specified according to the experimental data.[17] Furthermore, the total mass flow of the vapor stream and the organic distillate (S4 and S10 in Figure 2) as well as the mass of catalyst and the catalyst activity (concentration of active sites) are specified. As autocatalytic reactions are negligible, the liquid hold-up in the reactive zone does not have to be specified in the simulations. The stage efficiency is set according to the values determined by independent measurements of the separation capacity.[17]

During the HCRD experiments of the butyl acetate system, the separation of the organic and the aqueous phase in the decanter was incomplete, so that aqueous phase was detected in the organic reflux. Hence, in this case, the decanter cannot be described satisfactorily by the equilibrium stage model as mentioned earlier. For that reason, different simulation modes are used for the butyl acetate and the hexyl acetate system. In the open simulation mode, which is used for the butyl acetate system, the HCRD column is cut free and simulated independently, so that the simulation of the decanter can be omitted. For that reason, temperature, pressure, and the component mass flows of the organic reflux (S8 in Figure 2) are specified additionally in the open simulation mode according to the experimental data.[17] In the closed simulation mode, which is used for the hexyl acetate system, the whole experimental set-up including the decanter and the condenser is simulated as described earlier, so that no additional specifications are necessary.

Due to low concentrations and low rates of formation, the side products and impurities are neglected and only the four main reactants (butanol, acetic acid, butyl acetate, and water or hexanol, acetic acid, hexyl acetate, and water, respectively) are considered in the simulations. For that reason, the sum of the mass fractions of these four main reactants is scaled to one.

General results

All simulations are carried out with the equation-oriented process simulator Chemasim (version 5.4.3.3), which is an in-house tool of BASF SE (Ludwigshafen, Germany). Note that the actual choice of the process simulator is not of importance. As only standard models are used in this work, any process simulator can be used. Tables 3 and 4 give an overview of the simulation results. The experimental and the simulation results of the mass fraction of acetate in the product stream and the conversion of acetic acid are compared for the synthesis of butyl acetate (open simulation mode; cf. Table 3) and the synthesis of hexyl acetate (closed simulation mode; cf. Table 4). The results from the synthesis of hexyl acetate show very good agreement between the simulations and the experiments. The maximum relative error of the predicted conversion and mass fraction of acetate in the product stream is 1.2% (cf. Table 4). The relative error of the predicted conversion and mass fraction of acetate in the product stream of the butyl acetate synthesis is generally between 0.6 and 3.0% (cf. Table 3). Hence, the differences

Table 3. Comparison of Selected Experimental and Simulation Results (Conversion of Acetic Acid X_{HAc}, Mass Fraction of Butyl Acetate in the Product Stream $x_{ButAc}^{(m),prod}$) As Well As Their Relative Deviations for the Butyl Acetate System (Open Simulation Mode)

	X_{HAc}			$x_{HexAc}^{(m),prod}$ (g/g)		
	Exp.	Sim.	Rel. Dev. (%)	Exp.	Sim.	Rel. Dev. (%)
But01	0.945	0.926 ± 0.019	2.1	0.965	0.942 ± 0.069	2.4
But02	0.881	0.895 ± 0.016	1.5	0.861	0.835 ± 0.082	3.0
But03	0.932	0.927 ± 0.011	0.6	0.953	0.937 ± 0.076	1.7
But04	0.927	0.920 ± 0.015	0.7	0.958	0.950 ± 0.055	0.8
But05	0.910	0.848 ± 0.092	6.9	0.986	0.971 ± 0.037	1.5
But06	0.953	0.931 ± 0.053	2.2	0.984	0.966 ± 0.054	1.8

Estimations of the maximum errors limit are given for the simulation results.

Table 4. Comparison of Selected Experimental and Simulation Results (Conversion of Acetic Acid X_{HAc}, Mass Fraction of Hexyl Acetate in the Product Stream $x_{HexAc}^{(m),prod}$) As Well As Their Relative Deviations for the Hexyl Acetate System (Closed Simulation Mode)

	X_{HAc}			$x_{\mathrm{HexAc}}^{(\mathrm{m}),\mathrm{prod}}$ (g/g)		
	Exp.	Sim.	Rel. Dev. (%)	Exp.	Sim.	Rel. Dev. (%)
Hex01	0.929	0.918 ± 0.019	1.2	0.979	0.970 ± 0.020	0.8
Hex02	0.930	0.937 ± 0.015	0.7	0.977	0.980 ± 0.019	0.3
Hex03	0.896	0.900 ± 0.020	0.5	0.943	0.946 ± 0.025	0.3
Hex04	0.925	0.933 ± 0.015	0.9	0.977	0.984 ± 0.017	0.6
Hex05	0.943	0.951 ± 0.016	0.8	0.995	0.996 ± 0.006	0.0

Estimations of the maximum errors limit are given for the simulation results.

between the experimental and the simulation results concerning the mass fraction of acetate in the product stream and the conversion are slightly larger for the butyl acetate system than for the hexyl acetate system. Only the predicted conversion of experiment But05 deviates by ~7%. This large relative error will be discussed in the following section.

Figures 4–7 depict comparisons of the experimental and the predicted liquid-phase concentration and temperature profiles of the experiments But04, But06, Hex02, and Hex05.[17] The maximum error limits indicated by the dark gray area in Figures 4–7 will be discussed in the following section. Note that there are two values for the liquid-phase concentration on each stage in the reactive zone. The first value (counted from the top of the column that is from the direction of the liquid flow) is the liquid concentration leaving the distillation tray, and the second value is the concentration after the catalyst bed reactor. The predicted concentration and temperature profiles are in excellent agreement for the hexyl acetate system (cf. Figures 6 and 7). Similar results are obtained for the other HCRD experiments of that test system. For the butyl acetate system, the predicted concentration and temperature profiles are in good agreement as well (cf. Figures 4 and 5). Only in some parts, somewhat larger differences between the simulation and the experimental results are observed, for example, at the lower end of the reactive zone in experiment But04 for the concentration of butanol and butyl acetate (cf. Figure 4). A possible explanation for these differences is discussed in the next section.

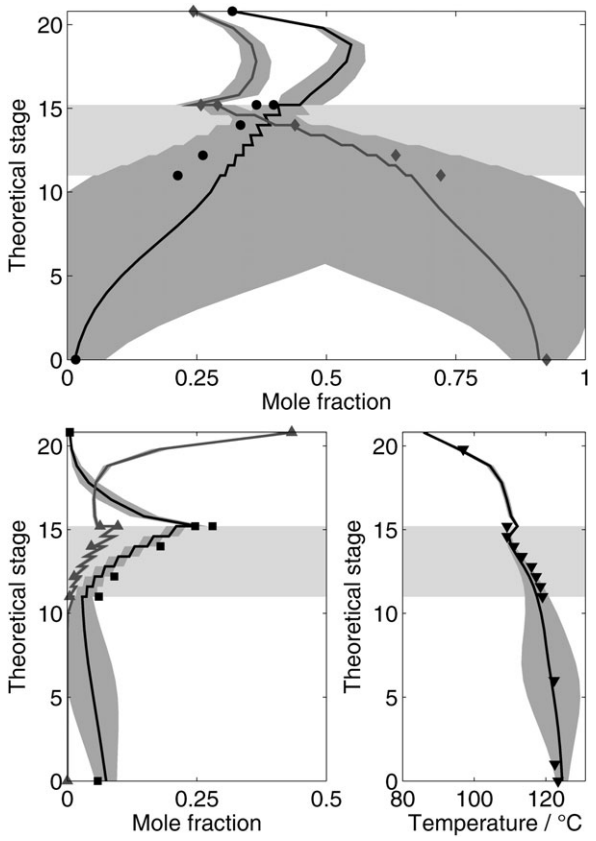

Figure 4. Liquid concentration (top and left) and temperature profiles (right) of experiment But04.

Comparison of experimental data (ButOH: ●, ButAc: ◆, HAc: ■, H_2O ▲, and temperature: ▼) with simulations (lines). Dark gray shaded area: maximum error limits due to errors in the input parameters. Light gray shaded area: location of the reactive zone.

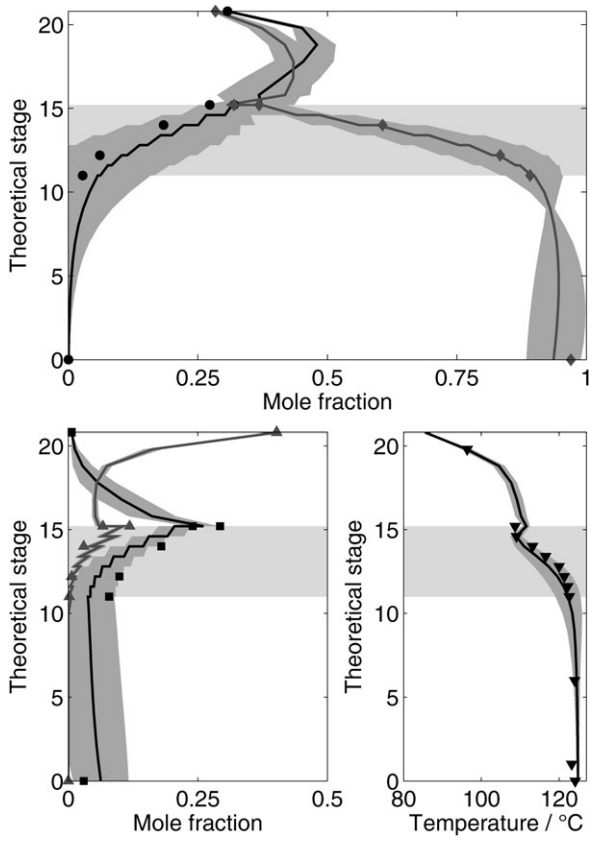

Figure 5. Liquid concentration (top and left) and temperature profiles (right) of experiment But06.

Comparison of experimental data (ButOH: ●, ButAc: ◆, HAc: ■, H_2O ▲, and temperature: ▼) with simulations (lines). Dark gray shaded area: maximum error limits due to errors in the input parameters. Light gray shaded area: location of the reactive zone.

Table 5. Overview of the Estimates for the Relative Errors of the Input Parameters

	Relative Error (%)	
	Butyl Acetate	Hexyl Acetate
Component mass flow		
Feed	1.0	1.0
Reflux (organic)	2.5	–
Total mass flow		
Distillate (organic)	–	0.5
Vapor stream	2.5	5.0
Pressure	0.3	0.5
Temperature	0.1	0.1
Stage efficiency	5.0	5.0
Catalyst capacity	5.0	5.0

Obviously, these differences in the concentration profiles do not affect the quality of the predicted overall conversion and mass fraction of acetate in the product stream (cf. Table 3). For the other HCRD experiments of the butyl acetate system, similar results are obtained. To conclude, the predictions generally describe the experiments well. Furthermore, it is emphasized that the simulation results presented here are fully predictive, as all parameters needed for the models are determined independently and are not fitted to the results of the HCRD experiments.

Sensitivity and error analysis

As experimental data are used as input parameters for the simulations (cf. "Input Parameters" section), the simulation results are inevitably affected by experimental errors. The experimental errors of the HCRD processes of this work are thoroughly discussed by von Harbou et al.[17] Considering the complete HCRD model as a vector function f with x as all input parameters and y as the output parameters, the error propagation can be estimated by Eq. 2.

$$\Delta y_{i,\max} = \left|\frac{\partial f_i}{\partial x_1}\right|\Delta x_1 + \left|\frac{\partial f_i}{\partial x_2}\right|\Delta x_2 + \ldots + \left|\frac{\partial f_i}{\partial x_n}\right|\Delta x_n \qquad (2)$$

In Eq. 2, Δx_j denotes the maximum error of the input parameter x_j. It is considered to be always positive. The derivative $\partial f_i/\partial x_j$ is the sensitivity of the output parameter y_i with respect to the input parameter x_j. $\Delta y_{i,\max}$ is the maximum error limit of the output parameter y_i. In this work, the sensitivities are calculated numerically by perturbation of the input parameter x_j using the simulation model presented earlier. The errors of the input parameters Δx_j are estimated from the experimental data, for example, from the variances of the measurements. Table 5 gives an overview of the relative errors of all input parameters. As both the mass of catalyst and the catalyst activity (concentration of active sites) occur in the model as prefactors for the rate of reaction, they can be lumped to a single factor called here catalyst capacity (number of active sites). It is assumed that the relative errors are constant for all experiments of one test system.

Discussion

The maximum error limits of the predicted conversion and mass fraction of acetate in the product stream are included for all experiments in Tables 3 and 4. The maximum error limits of the predicted concentration and temperature profiles are indicated by the dark gray areas in Figures 4–7 for the experiments But04, But06, Hex02, and Hex05. Note that the maximum error limits are worst-case estimations.

The differences between the predictions by simulation and the experimental results are clearly within the maximum error limits both for the conversion and mass fraction of acetate in the product streams (cf. Tables 3 and 4) as well as for the concentration and temperature profiles (cf. Figures 4–7). Typically, in those parts of the column where the differences between the predicted and the experimental concentration or temperature profiles are relatively large, the predicted error limits are large as well, see, for example, the concentration profile of butanol at the lower end of the reactive zone for experiment But04 shown in Figure 4. Furthermore, the maximum error limits of the concentration and temperature profiles are generally larger for the HCRD experiments of the butyl acetate system than for the HCRD experiments of the hexyl acetate system. This difference results from the different simulation modes that were used, and it will be discussed in more detail later.

The HCRD experiments But01–But06 and Hex01–Hex05, respectively, differ in the input parameters like the feed rate and the mass of catalyst (for values, see von Harbou et al.[17]). The comparison of the simulation results for the different experiments shows that the maximum error limits are not constant for one test system but depends strongly on the input parameters. For example, the sensitivity and error analysis predicts the largest error limit of the conversion for the experiment But05 (cf. Table 3). This large error limit is explained by the low absolute amount of acetic acid in the

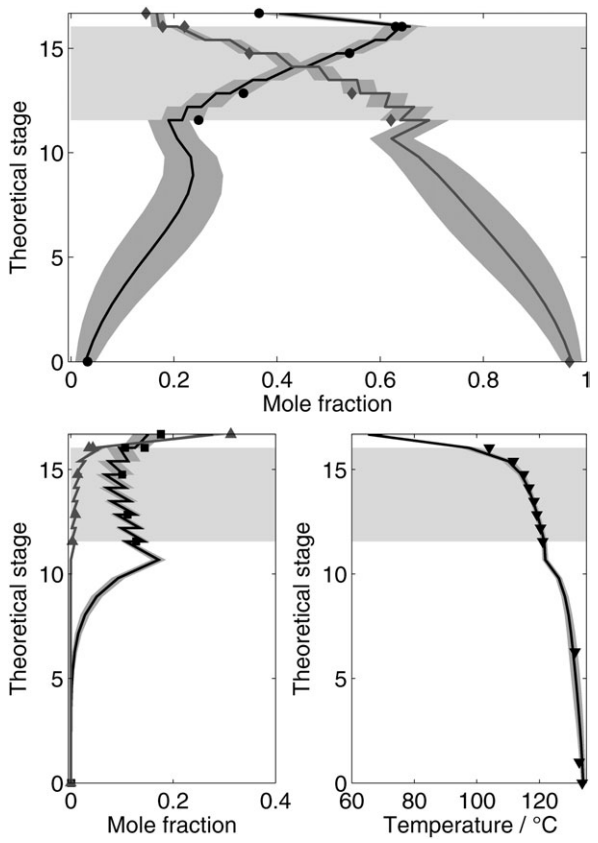

Figure 6. Liquid concentration (top and left) and temperature profiles (right) of experiment Hex02.

Comparison of experimental data (HexOH: ●, HexAc: ◆, HAc: ■, H_2O ▲, and temperature: ▼) with simulations (lines). Dark gray shaded area: maximum error limits due to errors in the input parameters. Light gray shaded area: location of the reactive zone.

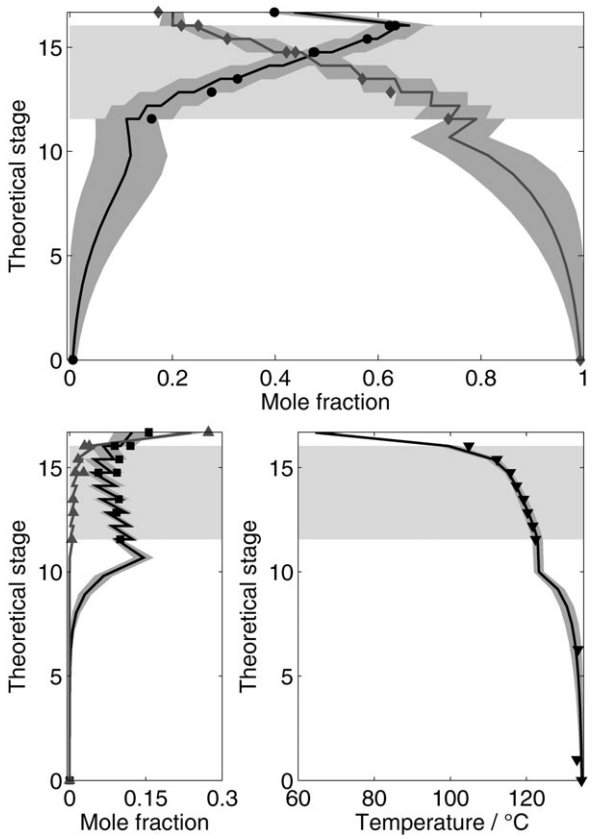

Figure 7. Liquid concentration (top and left) and temperature profiles (right) of experiment Hex05.

Comparison of experimental data (HexOH: ●, HexAc: ◆, HAc: ■, H_2O ▲, and temperature: ▼) with simulations (lines). Dark gray shaded area: maximum error limits due to errors in the input parameters. Light gray shaded area: location of the reactive zone.

feed of that experiment, which was about a factor of three lower than in the other experiments. Thus, it is not surprising that the difference between the predicted and the measured conversion is the largest for the experiment But05.

The HCRD experiments But04 and But06, and Hex02 and Hex05, of which the concentration and temperature profiles are shown in Figures 4–7, differ mainly in the amount of catalyst installed in the reactive zone of the HCRD column. Both in experiment But06 and in experiment Hex05, the amount of catalyst and thus the ratio of catalyst to feed load were increased by 68 and 44%, respectively, compared with the base case experiments But04 and Hex02.[17] By comparing Figure 4 with Figure 5 and Figure 6 with Figure 7, the differences in the maximum error limits due to variations of the input parameters become obvious. Using the example of the input parameter ratio of catalyst to feed load, the strong influence of the input parameters on the maximum error limits is demonstrated in the following. For that purpose, the ratio of catalyst to feed load is systematically varied in the same range as in the HCRD experiments.[17] All other input parameters are kept constant according to the data of the base case experiments But04 and Hex02, respectively. For each set of input parameters, the maximum error limits are estimated by simulations as described earlier. Figures 8 and 9 depict the maximum error limits for three important output parameters, namely, the conversion of acetic acid, the mole fraction of acetate in the product stream, and the mole fraction of acetate on the bottom most D +R tray as a function of the ratio of catalyst to feed load. In addition, it is shown in Figures 8 and 9 how the uncertainties in different input parameters contribute to the maximum error limits of the considered three output parameters. Here, only the significant error contributions are shown, that is, the error contributions of the input parameters mass flow of the feed stream, catalyst capacity, mass flow of the vapor stream, and mass flow of the organic reflux. As described earlier, the error limits are generally larger for the butyl acetate system (cf. Figure 8) than for the hexyl acetate system (cf. Figure 9). Depending on the ratio of catalyst to feed load, error contributions of different input parameters are predominant. For example, at a low ratio of catalyst to feed load, which correspond to a short residence time in the catalyst bed, the influence of an error in the catalyst capacity (mass of catalyst and concentration of active sites) is predominant (see top part of Figures 8 and 9). In contrast, at a high ratio of catalyst to feed load, which means that the conversion over the catalyst beds reaches the equilibrium conversion, the influence of the error in the catalyst capacity is negligible, as expected.

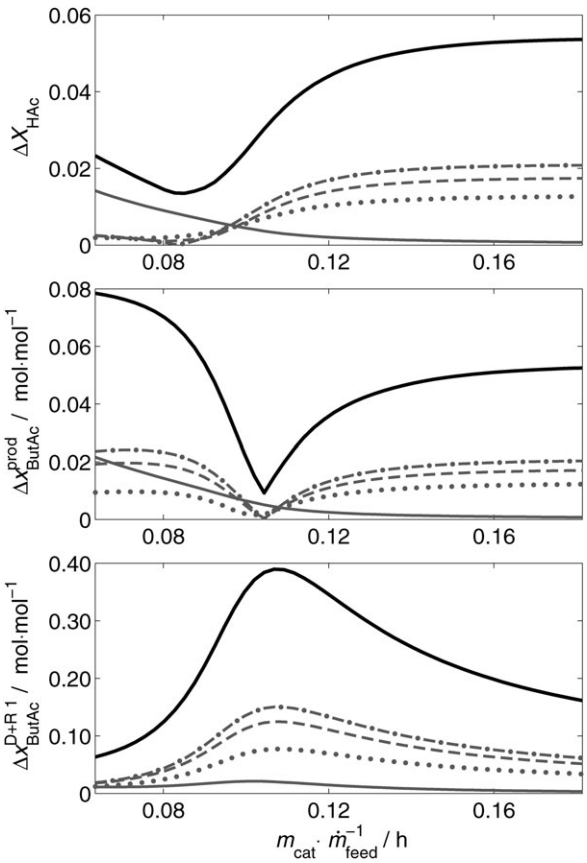

Figure 8. Estimation of the maximum error limits of the conversion of acetic acid (top), the mole fraction of butyl acetate in the product stream (middle), and the mole fraction of butyl acetate on the bottom most D + R tray (bottom) as a function of the ratio catalyst to feed load for the butyl acetate system.

The remaining input parameters are specified according to experiment But04. Error contributions (gray lines): mass flow of the feed stream (· · ·), catalyst capacity (—), mass flow of the vapor stream (· –), and mass flow of organic reflux (– –). Total maximum error limit (black solid line).

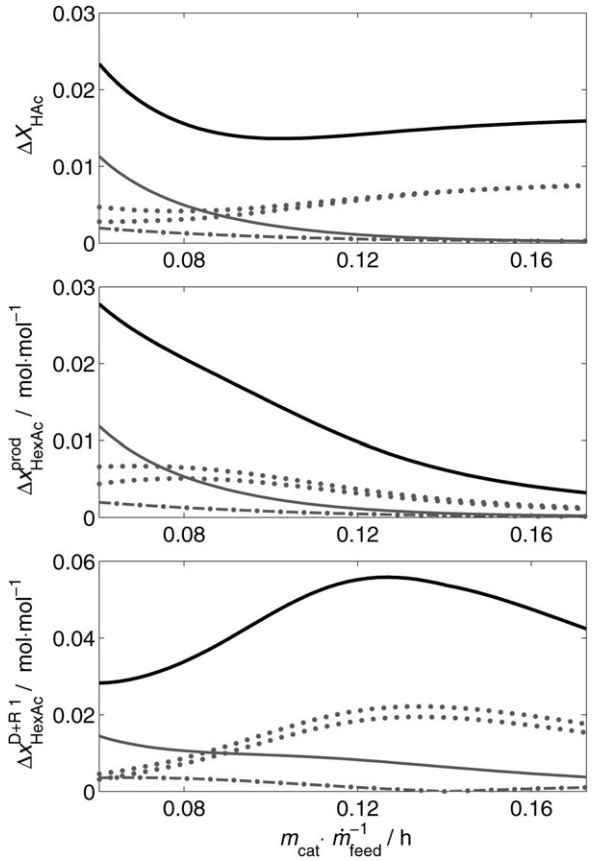

Figure 9. Estimation of the maximum error limits of the conversion of acetic acid (top), the mole fraction of hexyl acetate in the product stream (middle), and the mole fraction of hexyl acetate on the bottommost D + R tray (bottom) as a function of the ratio catalyst to feed load for the hexyl acetate system.

The remaining input parameters are specified according to experiment Hex02. Error contributions (gray lines): mass flows of the two feed streams (· · ·), catalyst capacity (—), and mass flow of the vapor stream (· –). Total maximum error limit (black solid line).

Furthermore, the differences between the open simulation mode (butyl acetate system) and the closed simulation mode (hexyl acetate system) become evident. In the closed simulation mode, for example, an error in the vapor stream mass flow has only a minor impact on the total maximum error limit (cf. Figure 9). In the open simulation mode, however, the error contribution of the vapor stream mass flow is for the most part predominant (cf. Figure 8). All mass flows apart from the bottom product mass flow (feeds, vapor stream, and reflux) are specified as input parameters in the open simulation mode. Although in the closed simulation mode, an error in the vapor stream mass flow can be compensated for by the reflux, in the open simulation mode, it affects directly the bottom product mass flow, which is the only unspecified mass flow, and it leads directly to a strong distortion of the concentration and temperature profiles.

To conclude, this error analysis predicts larger maximum error limits for the butyl acetate system than for the hexyl acetate system. The differences between the experimental and the simulation results, which are more pronounced for the butyl acetate system than for the hexyl acetate system, can be explained by the propagation of small errors in the input parameters. The results, hence, indicate that the HCRD model is suited for predicting the experiments. They also show that the experiments are consistent and of high quality.

Conclusions

A simulation study of a new type of laboratory equipment for HCRD experiments, the D + R tray, is presented. The special design of the D + R tray enables the straightforward characterization of the D + R tray both as a reactor and as a distillation unit, resulting in a simple and physically reasonable model of the D + R tray. The model is based on an equilibrium stage model to describe the distillation and a PFR model (series of CSTRs) implemented as side reactor to describe the catalyst bed reactor. The predictive simulation results are compared with data from HCRD experiments. In general, the simulation and the experimental results are in good agreement. For the hexyl acetate system, the simulations predict the experimental results (e.g., conversion, product composition, and concentration and temperature profiles) almost perfectly. In the butyl acetate system, however, in some parts larger differences between the predicted and experimental data are observed than in the hexyl acetate system. These larger differences are explained by a sensitivity and error analysis carried out for the HCRD experiments of both test systems. The differences between the simulation and experimental results occurring in the butyl acetate system can be explained by the propagation of small errors in the input parameters. The error analysis, hence, confirms both the experimental data and the model.

The fact that the D + R tray can be described by a simple and physically reasonable model, which can be easily implemented in a commercial process simulator and which is able to predict reliably the results from HCRD experiments, demonstrates the usefulness of the D + R tray for studying HCRD processes in the laboratory scale.

Notation

Bo = Bodenstein number
D = direction matrix
$\dot{m}$ = mass flow
M_i = molar mass of component i
m_{cat} = mass of catalyst
M_{meas} = number of measurements
N_{CSTR} = number of CSTRs in series
S = standard deviation
w = weight
x = vector of input parameters
X_i = conversion of component i
x_i = mole fraction of component i
Δx_i = maximum error of the input parameter x_i
$x_i^{(m)}$ = mass fraction of component i
y = vector of output parameters
Δy_i = maximum error limit of the output parameter y_i
z = reconciled value
$\tilde{z}$ = measured value

Greek letters

$\nu_{i,j}$ = stoichiometric coefficient of component i in reaction j
$\dot{\xi}_j$ = extent of reaction j
Ω = weighted sum of squared errors

Superscripts and subscripts

ButAc = *n*-butyl acetate
cat = catalyst
HAc = acetic acid
HexAc = *n*-hexyl acetate
meas = measured
prod = product

Literature Cited

1. Taylor R, Krishna R. Modelling reactive distillation. *Chem Eng Sci*. 2000;55(22):5183–5229.
2. Hiwale RS, Bhate NV, Mahajan YS, Mahajani SM. Industrial applications of reactive distillation: recent trends (Review). *Int J Chem React Eng*. 2004;2:1–52.
3. Sharma MM, Mahajani S. *Industrial applications of reactive distillation*. In: Sundmacher K, Kienle A, editors. *Reactive Distillation*. Weinheim, Germany: Wiley-VCH, 2003:3–29.
4. Taylor R. (Di)still modelling after all these years: a view of the state of art. In: *Proceedings of the IChemE Symposium, Series No. 152, Distillation & Absorption 2006, London, UK*, 2006.
5. Krishna R. *Hardware Selection and design aspects for reactive distillation columns*. In: Sundmacher K, Kienle A, editors. *Reactive Distillation*. Weinheim, Germany: Wiley-VCH, 2003:169–189.
6. Dörhöfer T. Gestaltung und Effektivität von Bodenkolonnen für die Reaktivrektifikation. Ph.D. thesis. Technische Universität München, 2006.
7. Buchaly C, Kreis P, Górak A. Hybrid separation processes—combination of reactive distillation with membrane separation. *Chem Eng Processing: Process Intensification*. 2007;46(9):790–799.
8. Buchaly C, Kreis P, Górak A. *n*-Propyl propionate synthesis via catalytic distillation—experimental investigation in pilot-scale. *Ind Eng Chem Res*. 2011;51(2):891–899.
9. Hanika J, Kolena J, Smejkal Q. Butylacetate via reactive distillation—modelling and experiment. *Chem Eng Sci*. 1999;54(21):5205–5209.
10. Pöpken T, Steinigeweg S, Gmehling J. Synthesis and hydrolysis of methyl acetate by reactive distillation using structured catalytic packings: experiments and simulation. *Ind Eng Chem Res*. 2001; 40(6):1566–1574.
11. Steinigeweg S, Gmehling J. *n*-Butyl acetate synthesis via reactive distillation: thermodynamic aspects, reaction kinetics, pilot-plant experiments, and simulation studies. *Ind Eng Chem Res*. 2002; 41(22):5483–5490.
12. Schmitt M, Hasse H, Althaus K, Schoenmakers H, Götze L, Moritz P. Synthesis of n-hexyl acetate by reactive distillation. *Chem Eng Process: Process Intensification*. 2004;43:397–409.
13. Parada S. Nebenreaktionen bei der heterogen katalysierten Reaktivdestillation am Beispiel der Herstellung von Butylacetat. Ph.D. thesis. Universität Stuttgart, 2008.
14. Moritz P, Hasse H. Fluid dynamics in reactive distillation packing Katapak-S. *Chem Eng Sci*. 1999;54(10):1367–1374.
15. Adrian T, Beßling B, Hallmann H, Niekerken J, Spindler V, Ohligschläger A, Rimpf M. German Patent No. DE 19860598 A1, 2000.
16. Schmitt M, von Harbou E, Parada S, Grossmann C, Hasse H. New equipment for laboratory studies of heterogeneously catalyzed reactive distillation. *Chem Eng Technol*. 2009;32(9):1313–1317.
17. von Harbou E, Schmitt M, Parada S, Grossmann C, Hasse H. Study of heterogeneously catalysed reactive distillation using the D+R tray—a novel type of laboratory equipment. *Chem Eng Res Des*. 2011;89(8):1271–1280.
18. Schladt M, Hu B. Soft sensors based on nonlinear steady-state data reconciliation in the process industry. *Chem Eng Process: Process Intensification*. 2007;46(11):1107–1115.
19. Keller T, Holtbruegge J, Górak A. Transesterification of dimethyl carbonate with ethanol in a pilot-scale reactive distillation column. *Chem Eng J*. 2012;180:309–322.
20. Blagov S, Parada S, Bailer O, Moritz P, Lam D, Weinand R, Hasse H. Influence of ion-exchange resin catalysts on side reactions of the esterification of *n*-Butanol with acetic acid. *Chem Eng Sci*. 2006; 61(2):753–765.
21. Grob S, Hasse H. Thermodynamics of phase and chemical equilibrium in a strongly nonideal esterification system. *J Chem Eng Data*. 2005;50(1):92–101.
22. Schmitt M, Hasse H. Chemical equilibrium and reaction kinetics of heterogeneously catalyzed *n*-hexyl acetate esterification. *Ind Eng Chem Res*. 2006;45(12):4123–4132.
23. Schmitt M, Hasse H. Phase equilibria for hexyl acetate reactive distillation. *J Chem Eng Data*. 2005;50(5):1677–1683.
24. von Harbou E. Experiments with novel equipment and morphological analysis of heterogeneously catalysed reactive distillation. Ph.D. thesis. University of Kaiserslautern, 2012.
25. King CJ. *Separation Processes*, 2nd ed. New York: McGraw-Hill Book Company, 1980.
26. Levenspiel O. *Chemical Reaction Engineering*, 3rd ed. Hoboken, USA: Wiley, 1999.
27. Schmitt M. Heterogen katalysierte Reaktivdestillation: Stoffdaten, Experimente, Simulation und Scale-up am Beispiel der Synthese von Hexylacetat. Ph.D. thesis. Universität Stuttgart, 2006.
28. Gmehling J, Kolbe B. *Thermodynamik*, 2nd ed. Weinheim, Germany: Wiley-VCH, 1992.
29. Narasimhan S. *Data Reconciliation & Gross Error Detection: an Intelligent Use of Process Data*. Houston, USA: Gulf Pub. Co., 2000.

Appendix: Implementation of the Data Reconciliation

The objective function Ω of the data reconciliation problem that was used in this work is given in Eq. A1.

$$\Omega = \sum_{i=1}^{M_{\text{meas}}} w_i (z_i - \tilde{z}_i)^2 \stackrel{!}{=} \min \tag{A1}$$

z_i refers to the reconciled value, $\tilde{z}_i$ to the value measured in the experiment, w_i to the weight, and M_{meas} to the total number of measured values. Different approaches exist to choose the measured values that are reconciled $\tilde{z}_i$, the weights w_i, and the physical constraints (for details see, e.g., Narasimhan[29]). In this work, the measured mass flows $\tilde{\dot{m}}_k$ and the measured mass fractions $\tilde{x}_{i,k}^{(\text{m})}$ are reconciled but not only of the input and output streams of the HCRD process but also of the organic reflux stream. For that reason, the whole HCRD set-up is divided into subunits, namely, the column, the condenser, the decanter, and the splitter (cf. Figure 2). The component mass balances of all components $i = 1\ldots N$ over all subunits $l = 1\ldots P$ and the summation conditions of the mass fractions (normalization equation) of all streams $k = 1\ldots S$ are used as constraints, see Eqs. A2 and A3. To account for the reactions $j = 1\ldots R$ (see "Chemical Systems" section) occurring in the column, the unknown extent of reaction $\dot{\xi}_j$ is introduced in the component mass balance.

$$0 = \sum_{k=1}^{S} D_{l,k} \cdot \dot{m}_k x_{i,k}^{(\text{m})} + C_l \cdot M_i \sum_{j=1}^{R} \nu_{i,j} \dot{\xi}_j \quad \text{with} \quad i = 1\ldots N; l = 1\ldots P \tag{A2}$$

$$1 = \sum_{i=1}^{N} x_{i,k}^{(\text{m})} \quad \text{with} \quad k = 1\ldots S \tag{A3}$$

In Eq. A2, $D_{l,k}$ denotes the (l,k)th-element of the direction matrix D. The direction matrix defines the direction of all streams (1: input, -1: output) for all subunits. C_l is an element of the catalyst vector C (1: subunit l contains catalyst, i.e., reactions take place, 0: no catalyst in subunit l). M_i refers to the molar mass of the component i and $\nu_{i,j}$ refers to the stoichiometric coefficient of component i in reaction j. The total number of components N in this work is seven: four main reactants, two by-products (see "Chemical Systems" section), and the rest, in which all unknown components are summarized, for example, impurities that are introduced into the process by the feed. To fulfil the condition of conservation of mass during reaction, it is important that the molar masses M_i fit exactly to the corresponding stoichiometric coefficients $\nu_{i,j}$ and satisfy Eq. A4. Otherwise, even small differences result in inconsistent component mass balances.[18]

$$\sum_{i=1}^{N} v_{i,j} \cdot M_i = 0 \quad \text{with} \quad j = 1 \ldots R \tag{A4}$$

The implementation of matrices in the component mass balances (cf. Eq. A2) is very useful, as it enables the quick adaptation of the data reconciliation problem to other set-ups and other reaction networks.

As a splitter was used in the HCRD experiments for the synthesis of hexyl acetate, the composition of the organic reflux stream and of the organic distillate stream (stream number 8 and 10 in Figure 2) have to be equal, yielding additional constraints, see Eq. A5.

$$0 = x_{i,8}^{(\mathrm{m})} - x_{i,10}^{(\mathrm{m})} \quad \text{with} \quad i = 1 \ldots N-1 \tag{A5}$$

The weights in Eq. A1 are important to reflect the accuracy of the respective measurement and to make the least squares independent of the dimension of the measurements. Narasimhan[29] suggests to define the weights on the basis of the standard deviations S_i of the measurements, see Eq. A6.

$$w_i = \frac{1}{S_i^2} \tag{A6}$$

The standard deviation of the mass flow $S_{\dot{m}_k}$ can be directly computed from repeated measurements. The standard deviations of the mass fractions $S_{x_i^{(\mathrm{m})}}$ are set according to the estimations of the errors, resulting in 0.01 g/g for the mass fractions of the main reactants and 0.05 g/g for the mass fractions of the remaining components. To avoid unfeasible values such as negative mass fraction, the values z_i are bounded. The boundaries are calculated according to Eqs. A7 and A8

$$\max(\dot{m}_k - \Delta\dot{m}_k, 0) \leq \dot{m}_k \leq (\dot{m}_k + \Delta\dot{m}_k) \tag{A7}$$

$$\max\left(x_{i,k}^{(\mathrm{m})} - \Delta x_{i,k}^{(\mathrm{m})}, 0\right) \leq x_{i,k}^{(\mathrm{m})} \leq \min\left(x_{i,k}^{(\mathrm{m})} + \Delta x_{i,k}^{(\mathrm{m})}, 1\right) \tag{A8}$$

The maximum allowed adjustment of the concentration $\Delta x_{i,k}^{(\mathrm{m})}$ was set to 0.01 g/g, and the maximum allowed adjustment of the mass flow $\Delta\dot{m}_k$ was set to 10% of its measured value. Because of the linear dependence of the reaction network of the hexyl acetate system defined in Reactions IV–VI) (Reaction VI together with the backward Reaction VII is equal to the forward Reaction IV), it is impossible to determine a unique solution of the extents of reaction $\dot{\xi}_j$ of all four reactions. To avoid that problem, the extent of Reaction VII is bounded to positive values.

Assuming that the measurement errors are only random errors and no gross errors, that is, the measured values $\tilde{z}_i$ are not biased, the reconciliation process yields a consistent and statistically most probable data set. A global test for gross errors was applied to verify this assumption. If the minimum objective function value $\Omega_{\min}$ exceeds the 95% quantile of the χ^2-distribution with the difference of the total number of measured values and the number of constraints as degrees of freedom, the reconcilation leads to large adjustments being made to the measured values and it is most likely that the measurements are biased, that is, a gross error is detected.[29] No gross error was detected by this global test for the data of all HCRD experiments But01–But06 and Hex01–Hex05 given by von Harbou et al.[17] The data reconciliation problem as defined in Eqs. A1–A8 was implemented in Matlab (product of MathWorks, Natick) and was solved for all mass flows $\dot{m}_k$, mass fractions $x_{i,k}^{(\mathrm{m})}$, and extents of reaction $\dot{\xi}_j$ using the solver fmincon, which is based on a trust-region algorithm.

Manuscript received July 22, 2012, and revision received Oct. 5, 2012.